RSCPublishing **Faraday Discussions**

# How charges separate: correlating disorder, free energy, and open-circuit voltage in organic photovoltaics

SCHOLARONE™
Manuscripts

# Journal Name

# How charges separate: correlating disorder, free energy, and open-circuit voltage in organic photovoltaics

Débora P. Mroczek,[a] Vladimir Lankevich,[b] and Eric R. Bittner[c]

In order for a photovoltaic cell to function, charge carriers produced by photoexcitation must fully dissociate and overcome their mutual Coulomb attraction to form free polarons. This becomes problematic in organic systems in which the low dielectric constant of the material portends a long separation distance between independent polaron pairs. In this paper, we discuss our recent efforts to correlate the role of density of states, entropy, configurational and energetic disorder to the open-circuit voltage, $V_{oc}$ of model type-II organic polymer photovoltaics. By comparing the results of a fully interacting lattice model to those predicted by a Wigner-Weisskopf type model we find that energetic disorder does play a significant role in determining the $V_{oc}$; however, mobility perpendicular to the interface plays the deciding role in the eventual fate of a charge-separated pair.

## 1 Introduction

The performance of an organic photovoltaic devices depends on successful charge-separation following photoexcitation, which in turn hinges upon whether or not the initial excitonic state has sufficient electronic or vibronic energy to overcome the Coulomb attraction between an electron and hole.[1–4] Whether this happens rapidly through "hot" excitonic states or through thermalized "cold" states has been a matter of considerable recent debate and the answer to this question contains information crucial for the design of highly efficient organic solar cells. "Hot excitons" are attributed to the prompt formation of mobile polarons observed in fullerene/polymer blends. While many groups argue that "hot excitons" are the main source of photocurrent, experiments conducted by Vandewal et al indicate that it is "cold excitons" i.e. thermalized excited states are the ones that give the predominant contribution to the photocurrent.

The dissociation of electron-hole pairs into free charge carriers is especially puzzling since it requires an electron and a hole to overcome the strong electrostatic attractions under seemingly unfavorable conditions. Heuristically, charge carriers are *free* when

thermal energy is comparable to the Coulombic attraction,

$$\frac{e^2}{4\pi\varepsilon_0\varepsilon r} \le k_B T, \tag{1}$$

where $e$ is the electron charge, $\varepsilon_0$ is the vacuum permitivity, $\varepsilon$ is a dielectric constant of the material and $r$ is the distance of separation between a charges. Due to the low dielectric constant ($\varepsilon = 2-4$) of organic materials typically used in OPVs, an electron finds itself with a 0.5 eV barrier to surmount, corresponding to the Coulomb capture radius of 15 to 28 nm. It is highly improbable that charges would be able move this distance before recombining; however, it has been observed that free charge carriers can be formed at separations of 4 nm on the femtosecond timescales.[5,6] Thus, a goal of our recent work has been to rectify both "hot" and "cold" exciton dissociation mechanisms within the context of a common theoretical model.

From thermodynamics, we can consider the dissociation in terms of the reversible work (i.e. Helmholtz energy) required to separate an electron from a hole to a given radius.

$$F(r) = U(r) - TS(r) = U(r) - k_B T \ln\Omega(r) \tag{2}$$

where $\Omega(r)$ is the the number of equivalent electron/hole states with separation $r$, $T$ is the absolute temperature, $k_B$ is the Boltzmann constant, $U(r)$ is the electron-hole interaction potential, and $S$ is the entropy of the electronic degrees of freedom.[7] For a single polymer chain, a $\pi-$electron that is confined to move along a single quasi-one-dimensional polymer chain has only one

[a] University of Houston, Department of Physics, Houston, TX.; E-mail:dpmroczek@Central.UH.EDU

[b] University of Houston, Department of Chemistry & Department of Physics, Houston, TX.; Present address: Rice University, Department of Chemistry

[c] Corresponding Author. University of Houston, Department of Chemistry & Department of Physics, Houston, TX.; E-mail: ebittner@central.uh.edu.
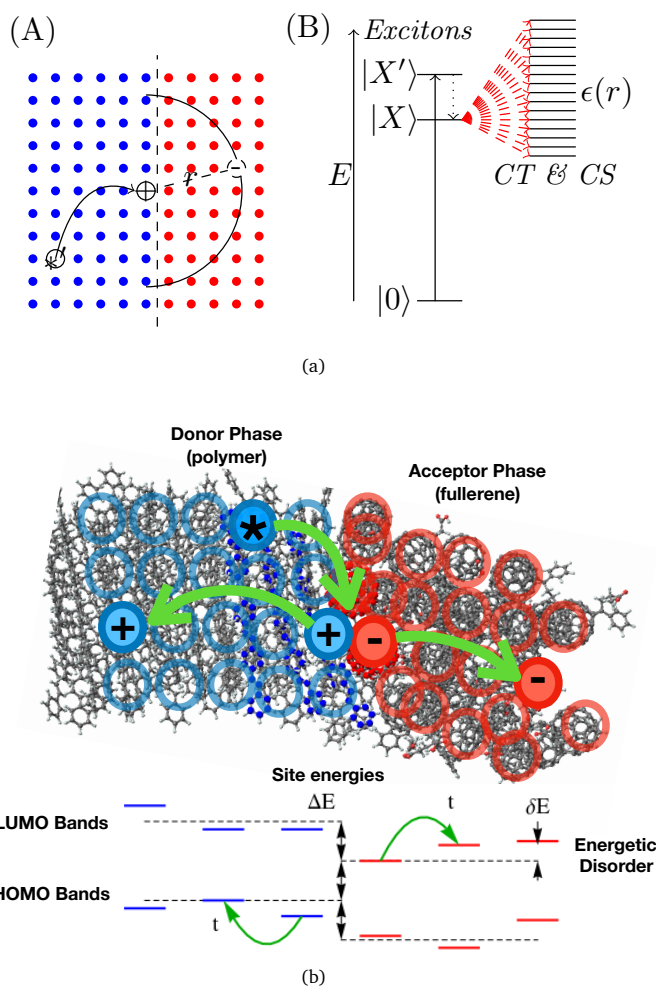
(a)



(b)

**Fig. 1** (a) Sketch of model. Our analytical model assumes that the hole remains pinned to the interface and that the donated charge tunnels some distance $r$ into the acceptor phase. While the sketch is in a two-dimensional plane, the full physical system and our calculations is in three-dimensions. (b) Atomistic representation of the interface and its mapping onto a site model that is represented as a set of two-level systems with energy gaps modulated about their average HOMO-LUMO gap.

defined path and consequently the electronic entropy contribution. For thin-films (2-D) and fullerene-based acceptors (3-D) the number of electron/hole configurations available to the system with a given electron/hole separation radius scales with the surface area

$$\Omega \propto (r/r_o)^{d-1}. \tag{3}$$

where $r_o$ is the unit length and $d = 1, 2, 3$ is the dimensionality of the system. Consequently the entropy

$$S = (d-1)\ln(r/r_o) \tag{4}$$

can become energetically comparable to the Coulombic energy of the electron-hole pair in two and three dimensions.[7,8] This has the desired result of providing a zero-work pathway for the dissociation of an exciton to a free electron/hole pair. This estimate, however, is only valid for the scenarios with an immobile hole.

Allowing the hole to move adds additional degrees of freedom and increases the number of available electronic states further emphasizing the importance of the entropic contribution. The reversible work theorem also implies an equality between chemical potential and the open-circuit voltage, $qV_{OC}$, of the photo-voltaic device[9] and establishes a crucial connection between theoretical and laboratory investigations of the current generation in OPVs. From such considerations, Burke *et al.* arrive at the following expression for the $V_{OC}$ from the canonical ensemble:

$$qV_{OC} = E_{CT} - \frac{\sigma_{CT}^2}{2k_BT} - k_BT\ln\left(\frac{qfN_0L}{\tau_{CT}J_{sc}}\right) \tag{5}$$

where $f$ is the volume fraction of the device that is mixed or interfacial, $L$ is the thickness of the solar cell, $J_{SC}$ is the short-circuit current of the cell, $q$ is the electronic charge, and $N_0$ is the density of the electronic states in the device. Equation 5 includes the necessary dependence of $qV_{OC}$, and therefore of $F$, on the average energy of the CT state, $E_{CT}$, disorder in the CT energies, expressed through standard deviation $\sigma_{CT}$, and the life-time of the CT-state, $\tau_{CT}$.[9] Nonetheless, this expression is composed of variables that refer to the entire device making Equation 5 difficult to connect to a microscopic model.

More recently, Hood and Kassal have shown that the free energy better reflects the energy landscape that an electron and a hole traverse, since the entropic term effectively lowers the energy barrier needed for the transferred charge to become a free charge carrier. Additional dissociation paths and energetic disorder make the Coulombic interaction comparable to the thermal fluctuations. Consequently, the Coulomb attraction no longer defines how far an electron and a hole can separate as suggested by Eq.1. Within the Hood and Kassal model, a bulk-heterojunction is an ensemble of energetically disordered hexagonal lattice sites. Under an assumption of electronic equilibrium, they then compute the free energy as[8]

$$F = -\langle k_BT\ln Z \rangle \tag{6}$$

where $Z$ is the partition function that describes specific energy states and the bracket $\langle\cdots\rangle$ denotes a statistical average over realizations of the disordered lattice. Both Equations 5 and 6 are

derived in the canonical ensemble and carry the same information. However, the latter approach is far more suitable for connecting to microscopic details such as energetic and structural disorder. There are, however, a few drawbacks of the Hood-Kassal model. The electrons and holes are not permitted to cross from one domain to the other, and a hole is restricted to move only perpendicular to the interface under the assumption of translational symmetry. The model includes the electrostatic potential, but does not take into account important quantum effects such as delocalization, mixing between excitonic and charge-transfer configurations, and electronic exchange effects.

We recently examined this approach using a fully interacting 2D electron/hole lattice model that our group developed for studying exciton and charge transfer dynamics at organic heterojunction interfaces [10–16] and compared it to experimental values for the open-circuit voltage by including site-energy disorder and thermal fluctuations within the lattice itself. We show that this generally facilitates charge separation; however, due to the excess energy supplied by the initial photoexcitation, highly energetic electron-hole pairs can dissociate in unfavorable directions, potentially never contributing to the photocurrent while "cold" thermalized states follow the free energy curve defined at the operating temperature of the device. [17] In this discussion, we pursue an heuristic/thermodynamical model that that can be solved analytically for computing the reversible work to separate charges at a given temperature. We find that the analytical model reproduces many of the features of a more detailed model in the limit of very low mobility of the transferred charge. We also explore the use of singular value decomposition of the electron/hole wave functions as a means to quantify when the separated carriers are truely independent.

## 2 Theoretical Models

### 2.1 Simple lattice model

We begin by considering a model donor/acceptor heterojunction system as sketched in Fig. 1 whereby the physical system is represented as a series of lattice points in three physical dimensions. The system is partitioned such that all points with $x < 0$ are considered to be in the Donor-phase while all points $x > 0$ are in the acceptor phase. Charge generation occurs when a neutral exciton, denoted as $*'$ in our sketch and created by photoexcitation, finds itself close to the phase boundary where there is sufficient driving force to separate the exciton into an electron/hole state. Within the context of our sketch, we will assume for purposes of this model that the vacated hole is either located at the origin or at some point $\vec{r}_o$ within the donor phase and the transferred electron is located at some lattice point $\vec{r}$ away from this site. This allows us to describe the resulting electron/hole configuration energy as $\varepsilon(r)$ which we will take to be

$$\varepsilon(r) = \Delta E - E_{off} + J(r) \qquad (7)$$

where $\varepsilon$ is the dielectric constant and $\Delta E$ is the energy gap between local LUMO and HOMO orbitals and $E_{off}$ is the offset between the HOMO orbitals in the acceptor phase and the HOMO orbitals in the Donor phase. For purposes of constructing a model

we can analyze analytically, we assume that the local site energy for an electron/hole configuration is Coulombic ($J = e^2/\varepsilon r$) at long range and and equal to the $U$ when the electron and hole are localized on the same site as in an excitonic configuration. Hence, $\varepsilon(0)$ corresponds to the energy of a non-dissociated exciton at the interface in our model. The interpolation between the local interaction $U$ and the long-range Coulomb interaction is given by the Mataga-Nishimoto potential

$$\varepsilon(r) = \frac{U}{1 + U\varepsilon_r r/r_o}. \qquad (8)$$

where $\varepsilon_r$ is the relative permittivity between the donor and acceptor materials (and can be set to 1 since we assume the two material to be conjugated organics) and $r_o = 14.397$ when distances are in Å and energies are in eV. Finally, we take the coupling between the exciton and the charge-separated states to be due to tunneling and of the form

$$v(r) = V_o e^{-\beta r} \qquad (9)$$

where $\beta^{-1}$ defines a tunnelling length. Within this model, the idempotent operator is given by

$$1 = |X\rangle\langle X| + \sum_r |r\rangle\langle r| \qquad (10)$$

where $|X\rangle$ denotes a local exciton state and $|r\rangle$ denotes a charge-separated state with electron/hole radius $r$. The energy eigenstates can be determined by expanding in this basis

$$|\mu\rangle = \langle\mu|X\rangle|\mu\rangle + \sum_r |r\rangle\langle r|\mu\rangle \qquad (11)$$

and then writing out the Hamiltonian matrix elements as

$$\varepsilon(r)\langle r|\mu\rangle + v(r)\langle X|\mu\rangle = E_\mu\langle r|\mu\rangle \qquad (12)$$

$$\sum_r v(r)\langle r|\mu\rangle = E_\mu\langle X|\mu\rangle. \qquad (13)$$

This leads to a transcendental equation for the energy eigenvalues,

$$E_\mu = \sum_r \frac{v^2(r)}{E_\mu - \varepsilon(r)}. \qquad (14)$$

Similarly, one finds the projection of the exciton onto the $|\mu\rangle$ eigenstate as

$$|\langle X|\mu\rangle|^2 = \left(1 + \sum_r \frac{v^2(r)}{(E_\mu - \varepsilon(r)^2)}\right)^{-1}. \qquad (15)$$

In the Wigner-Weiskopf model, one sets $\varepsilon(r) = r$ corresponding to a uniform density of states and assumes the coupling is constant. This allows both summations to be performed analytically. For the case at hand, we assume the sums can be transformed into radial integrations and then use the Laplace method to evaluate.
*

---

* While the model can be solved fully analytically, it is computationally far faster to simply diagonalize the Hamiltonian matrix given by Eqs. 12 and 13.
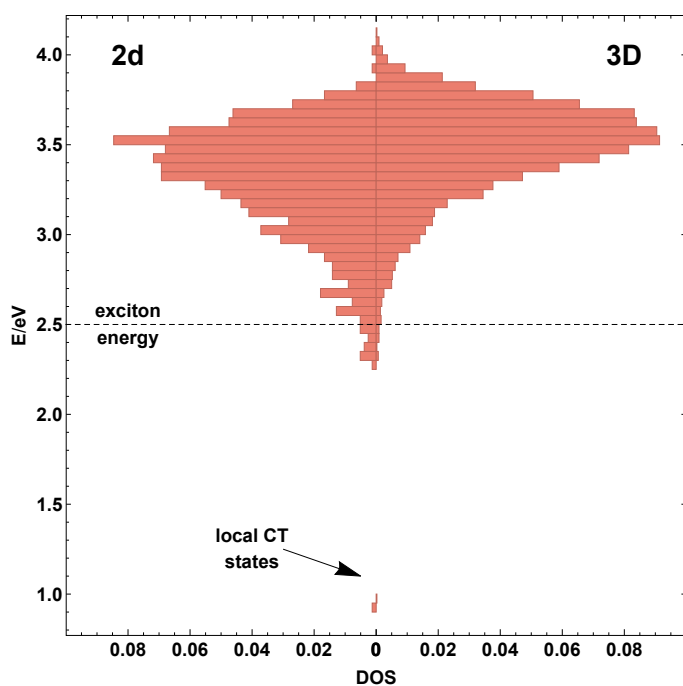
**Fig. 2** Normalized DOS for 2D and 3D model lattices.

For comparison, we consider the case of a 2D and a 3D lattice with similar parameters: $\{E_x \to 2.5eV, E_o \to 5eV, V_o \to -1eV, U \to 3eV, \beta \to 0.75^{-1}\}$ where $E_x = E_{D,lumo} - E_{D,homo} - U$ is the local exciton energy taken as the energy difference between the donor's LUMO and HOMO orbitals plus the local electron/hole attraction $U$, and $E_o = E_{A,lumo} - E_{D,homo}$ is the energy for a non-interacting electron/hole pair. Finally, we set the local electron/hole site energy to be

$$E(\vec{r}) = E_o + \varepsilon(r) + \delta E \tag{16}$$

with $\langle \delta E \rangle = 0$ and $\sqrt{\langle \delta E^2 \rangle} = 0.1eV$ to account for the fact that the local electron/hole site energies are distributed about $E_o$ to reflect inhomogeneous local environments. While the model is very simple and ignore interactions between charge-separated configurations, the resulting energies and density of states are similar to what we obtain with our more elaborate, fully interacting model, supporting that this heuristic model captures the salient physics of a more sophisticated model. Parametrically, the model presented here is identical to the more realistic, fully interacting heterojunction model we have published extensively upon over the past 15 years. We shall comment further on this model later in this report.

It is interesting to note that in the 2D case, there are far *more* states below the exciton energy (at $E = 0$) than above, which suggests that dimensionality plays a central role in the dissociation of an initially prepared exciton state. This notion is further enforced when we do a head-to-head comparison of the normalized density of states for the 2D and 3D lattices as shown in Figure 2. First, we note that the DOS in the 3D lattice is skewed towards higher energies as compared to the 2D lattice. Furthermore, in 3D the number of local charge-transfer states with energy lower than the exciton's energy is lower than in the 2D case. From this

simple model, we are drawn to the conclusion that dimensionality and density of states are every bit as important as energetics when building models for exciton dissociation.

Having determined the eigenstates of the model, we next construct a function describing the free energy required to separate charges to a given radius, $r_{sep}$. From statistical mechanics, we know that

$$F = -k_B T \ln Z \tag{17}$$

where $Z$ is the canonical partition function given in the usual way via summing over states

$$Z = \sum_\mu \exp(-E_\mu/k_B T). \tag{18}$$

We write this as an integral over $r$ and define $E_\mu(r)$ as the energy of a charge-separated state whose mean radius is equal to $r = |\langle \mu|\vec{r}|\mu \rangle|$. Thus

$$Z = \int_0^\infty g(r) \exp(-E_\mu(r)/k_B T) dr \tag{19}$$

where $g(r)$ the density of eigenstates with mean radius $r$. In Figure 3 we show that $E_\mu(r)$ can be described as a nearly single-valued function of $r$ except in cases where the exciton is resonant with the separation energy. Moreover, to a good approximation, $E_\mu(r) \approx \varepsilon(r)$ when we shift the spectral range to place the lowest energy eigenvalue at the origin with $r = 1$ and shift the interaction energy $\varepsilon(1) = 0$. This shift in the energy origin is typically done when constructing the partition function so that all energies are considered to be excitations from lowest energy state. Thus, we define the "radial" partition function and free energy as simply

$$Z_{ct}(r) = \exp(-(\varepsilon(r) - k_B T \ln(g(r)))/k_B T) \tag{20}$$

and

$$F_{ct}(r) = \varepsilon(r) - k_B T \ln(g(r))) \tag{21}$$

Taking $g(r) = 4\pi r^2$ as the 3D radial volume element we have an analytical expression for the free energy of a charge-separated state with radius $r$. Finally, the initial exciton state has an entropy of zero since it is a local state within our initial basis, and we write the reversible work as

$$\Delta F(r) = F_{ct}(r) - E_{ex}. \tag{22}$$

Finally, we introduce a correction for the relative kinetic energy of the charge-transfer state as function of the electron/hole separation radius. This can be justified from simple argument based on the uncertainty principle $\Delta x \Delta p \geq \hbar/2$ and $\langle K \rangle = \langle \Delta p^2 \rangle/2m$ which immediately yields that $\langle K \rangle \approx \hbar^2/(2mr^2)$ upon taking $r^2 = \langle \Delta x^2 \rangle$.

In Figure 3 we show compare the distribution of free energies compared to the electron/hole site energy, $\varepsilon(r)$ and the $F_{ct}$ as computed by Eq. 21, superimposed in white and red respectively. The dashed red-line includes the short-ranged kinetic energy correction which does appear to limit the closest point of contact between the electron and hole, but dies off rapidly at long distances. Further, to a good approximation, the free energy is well
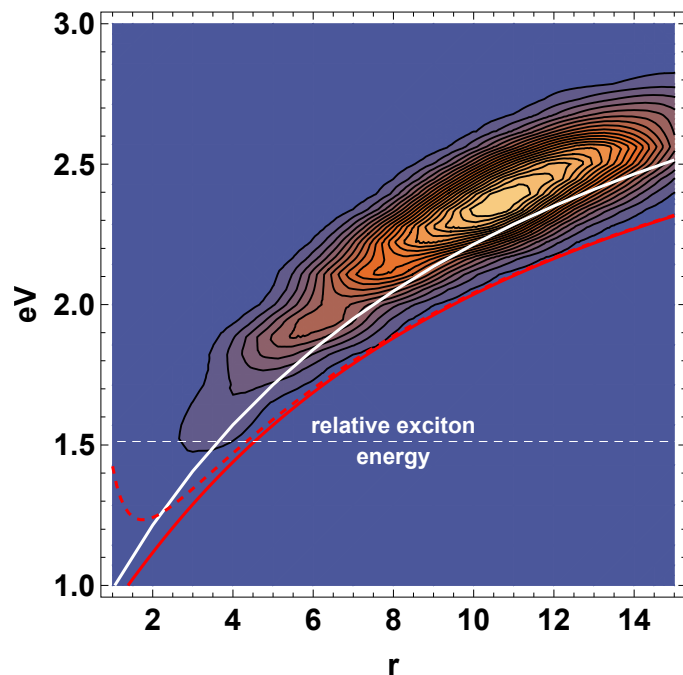
**Fig. 3** Energetics and approximate free energy from the Statistical Hopping model for exciton dissociation. The contours give the density of eigenstates with a given average electron/hole separation radius and eigenvalue energy. The white, red, and red-dashed curves are theoretical models of for the energy and free energy as described in the text.

approximated by simply the charge-transfer site energy $\varepsilon(r)$ and shows no indication of rolling over at ranges relevant for exciton dissociation. We conclude from this that models that do not allow the electron and hole to move independently and quantum mechanically or only include intermediate hopping or tunneling effects are poor representations of a semiconductor interfaces.

## 2.2  A Fully Interacting Model

Missing from this simple model is the fact that both the electron and the hole are both mobile and consequently are delocalized over multiple sites. Also, different electron/hole configurations interact. With these in mind, we next describe a fully interacting electron/hole model. Adding the additional degrees of freedom dramatically increases the complexity of the model, and hence the model is currently restricted to a 2D lattce. We recently used this model to assess the free energy of a 2D model heterojunction system[17] and we shall recapitulate some of the results here as they pertain to the heuristic model we presented above.

The model is described by the following electron/hole-+-

phonon Hamiltonian,[10,15]

$$\hat{H} = \hat{H}_{el} + \hat{H}_{el-ph} + \hat{H}_{ph}$$

$$= \sum_{\mathbf{mn}} (F_{\mathbf{mn}} + V_{\mathbf{mn}}) |\mathbf{m}\rangle \langle \mathbf{n}|$$

$$+ \sum_{\mathbf{mn},a,\mu} \left( \frac{\partial F_{\mathbf{mn}}}{\partial q_{a,\mu}} \right) q_{a,\mu} |\mathbf{m}\rangle \langle \mathbf{n}| \qquad (23)$$

$$+ \frac{1}{2} \sum_{\mu,a} \omega_a^2 (q_{a,\mu}^2 + \lambda q_{a,\mu,\mu+1}) + p_{a,\mu}^2,$$

where electron-hole configurations $|\mathbf{n}\rangle = |\mathbf{h}_i \mathbf{e}_j\rangle$ whereby a hole in a valence orbital on site $i$ and an electron in a conduction orbital on site $j$ form the basis for the Hamiltonian. We have published the details and parameterization of the model previously and, we briefly review its salient features. The term $F_{\mathbf{mn}}$ describes the single-particle motion for a non-interacting electron/hole pair. In its simplest form for configurations $|\mathbf{n}\rangle = |\mathbf{h}_i \mathbf{e}_j\rangle$ and $|\mathbf{m}\rangle = |\mathbf{h}_k \mathbf{e}_l\rangle$ it is given by

$$F_{\mathbf{mn}} = f_{jl}^e \, \delta_{ik} + f_{ik}^h \, \delta_{jl} \qquad (24)$$

where $f^e$ and $f^h$ have the meaning of localized energy levels and transfer integrals for conduction band electrons and valence band holes. In the absence of disorder, these quantities obey charge-conjugation symmetry with $f_{mn}^h = -f_{mn}^e$ and we assume that only nearest neighbors on the 2D lattice are coupled by these terms ($t = f_{i,i+1}$). The donor and acceptor domains are differentiated by imposing an energetic off-set, $\Delta E$, in the site-energies at the domain boundary as sketched in Fig. 1b. $V_{\mathbf{mn}}$ describes spin-dependent two-particle Coulombic and exchange interactions for each configuration, as well as interactions between different singlet geminate electron-hole pairs. For the case of singlet excitations,

$$V_{\mathbf{mn}} = -\langle h_i e_j | V | h_i e_j \rangle + 2\langle h_j e_i | V | h_i e_j \rangle. \qquad (25)$$

We assume that the inter-unit overlap of the primitive site-basis functions is small and that three types of integrals contribute to this interaction, each with well known meaning and long-range behavior.[10] First, an electron and hole on sites separated by a distance $r$ will experience a long-range Coulomb attraction of the Mataga-type as used above

$$\langle h_i e_j | v | h_i e_j \rangle = \frac{J_o}{1 + r_{ij}/r_o}, \qquad (26)$$

a short range exchange term which decays exponentially with electron/hole separation

$$\langle h_j e_i | v | h_i e_j \rangle = K_o \exp(-r_{ij}/r_o). \qquad (27)$$

Secondly, because differential overlap between an electron and hole sitting on the same site is substantial, we include the transition dipole-dipole coupling between singlet geminate electron hole pairs,

$$\langle h_i e_i | v | h_j e_j \rangle = \frac{D_o}{(r_{ij}/r_o)^3}. \qquad (28)$$

where $J_0$ and $K_0$ indicate Coulombic and exchange interactions between an electron and a hole on the same site. $D_0$ is a dipole moment of an electron-hole pair located on site $i$. It is important to note that these terms carry information pertaining to the spatial disorder in our model. While the model can treat singlet or triplet states, we are analyzing post-photoexcitation charge-transfer states and will only focus on singlets in this study.

The phonon term, $\hat{H}_{ph}$, assigns to each lattice site a high and a low frequency vibrational mode described by a local harmonic oscillator with weak nearest-neighbor coupling. These terms are determined from spectroscopic Huang-Rhys parameters typifying organic conjugated polymer systems. Such contributions modulate *both* the on-site band-gap as well as the site-to-site hopping integrals.

For a given lattice configuration, the eigenstates of the Hamiltonian in Eq. 23 are linear combinations of all configurations allowed on a particular lattice

$$(\hat{H}_{el} + \hat{H}_{el-ph}(\{\mathbf{q}\}))|\psi^k\rangle = E_k(\{\mathbf{q}\})|\psi^k\rangle \qquad (29)$$

with the $k$-th eigenstate defined as $|\psi^k\rangle = \sum_{ij} c_{ij}^k |h_i e_j\rangle$. We construct a 10 site $\times$ 10 site lattice with a donor-acceptor energy offset of $\Delta E = 0.5$ eV, the transfer energy between nearest sites set to $t = 0.536$ eV and lattice constant $a = 1$ nm in all directions. We deliberately choose a higher value for the hopping parameter (previously calculated to represent polymer intra-chain transfer energy[15]) to allow an electron and a hole easy passage throughout the lattice and to insure that nothing but the presence of disorder inhibits or facilitates electron/hole dissociation.

Since the fully interacting model allows valance holes in the acceptor region and conduction electrons in the donor domain, we need to be careful when defining the free energy as a function of electron/hole separation distance since we only want to include states in which the conduction electron is in the acceptor domain and the hole is in the donor domain. With this in mind, we define this as

$$\langle R_D^k \rangle = \sum_{ij} |\rho_{ij}^k| \vec{r}_{ij} \cdot \vec{n} \qquad (30)$$

where $\rho_{ij}^k$ is the eigenstate amplitude at electron/hole configuration and $\vec{n}$ is a unit vector normal to the donor/acceptor interface. The dotted curves in Figure 4 show the distribution of charge-transfer energies vs. mean electron/hoie separation radius $R_D$ as averaged over 1000 realizations of the site energies with a $\delta E = 0.01 eV - 0.20 eV$ fluctuation in the local site energy. The solid curves are the free energies which include the density of states contribution at 300K. Lastly, the shaded region indicates a range of literature values for $qV_{oc}$ for a variety of polymer/fullerene based heterojunction systems. This figure provides a connection between the "hot" and "cold" dissociation mechanisms for exciton dissociation.

One can think of a "hot" exciton process as occurring on a potential energy surface described by the average CT energy (i.e. the dotted curve in Figure 4. In this case, an exciton is injected into the system at an energy above $\approx 2.0 eV$. While some energetic relaxation may occur, the system encounters a small barrier
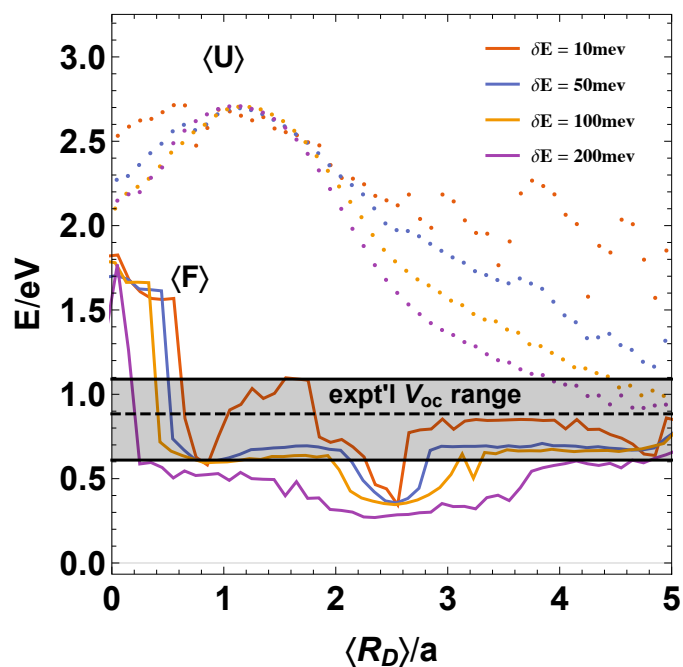


**Fig. 4** Average (points) and free energy (solid) curves for the fully-interacting model at different values of site-energy disorder $\delta E$. Shaded region represents the range of experimental values for open-circuit voltage with the average indicated by the dashed black line.

and can efficiently dissociate into separate charge-carriers. In this case, energy fluctuations appear to increase the effective energy barrier between the initial exciton at $R_D = 0$ and the fully separated charge carriers. Conversely, the "cold" exciton pathway can be understood as following a potential of mean force path along the free-energy minimum plotted as the solid curves. While the energy landscape is somewhat bumpy compare to the "hot" dissociation path, free energy fluctuations tend to be smoothen out by increasing the fluctuations in the site energies. In both cases the energetics converge to the experimental $qV_{oc}$ range. This leads to the ecumenical conclusion that both "hot" and "cold" exciton mechanisms contribute to the final production of charge-carriers.

In Figures 5(a-d) we present what happens when we modify the lattice model such that the transferred electron is far less mobile in the direction perpendicular to the interface than in the direction parallel to the interface. In this, we model more closely the case of $\pi$-stacked oligomers in the acceptor phase. The total energy and free energy curves are superimposed over the density of eigenstates in which the local site HOMO/LUMO gap included a random (static) fluctuation about a mean gap. The computed results reproduce many of the features of the exact model presented in Sec. 2.1 including the short-range kinetic energy contribution and the long-range tail of the average energy and free energy. This would imply that lower mobility in one of the phases has a profound impact on the ability of charges to escape from the interfacial region. Only in the instances of higher energetic disorder do we begin to see the free energy contribution begin to roll-over and plateau suggesting that local trapped states may facilitate the separation process.
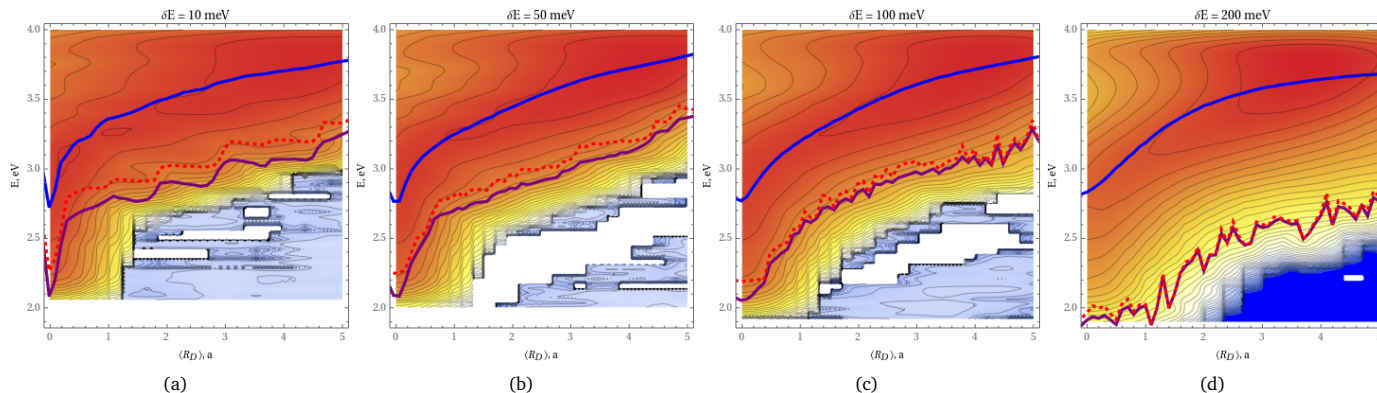
**Fig. 5** Radial energy distributions for lattice model with decreased mobility perpendicular to interface. The blue curve represents thermodynamic energy in the high temperature regime as a function of electron-hole separation; the dashed red curve is thermodynamic energy at 298 K; the purple curve is the free energy at 298 K. Contours and back-ground color indicate the normalized probability to find an eigenstate with a given energy and with a given electron/hole separation as sampled over fluctuations in the local site energies. In these cases we model the donor phases as a series of $\pi$-stacked oligomers with high electron/hole mobility parallel to the interface and much lower perpendicular to the interface. Both the total energy and free energies at $T = 300K$ are similar to the model of Sec. 2.1 where the transferred charge is effectively immobile.

## 2.3 Transition rates between states

In computing the eigenstates of Eq. 23 we took $q_{au} = 0$ and considered only the vertical excitations, assuming that fluctuations in the energy are due to the local electrostatics and not due to fluctuations in the phonons from their equilibrium positions. The remaining two terms in Eq. 23 allow for transitions between eigenstates. For this, we allow for both high and low-frequency phonon branches and assume that the coupling term $(\partial F_{nm}/\partial q_{a,\mu})$ can be determined from spectroscopic Huang-Rhys factors. It is then a simple matter to derive the golden-rule rate constant between eigenstates of $H_{el}|k\rangle = \varepsilon_k|k\rangle$ For this, we first perform a unitary (polaron/shift) transform on the entire $H$.[18]

$$\tilde{H} = e^{-S}He^{S} \tag{31}$$

where $S$ is an anti-hermitian operator

$$S = -\sum_{ka}(g_{kkq}/\omega_q)|k\rangle\langle k|(a_q^\dagger - a_q) \tag{32}$$

which gives that

$$e^{S} = \sum_{k}|k\rangle\langle k|\exp\left[-\sum_{q}\frac{g_{kkq}}{\omega_q}(a_q^\dagger - a_q)\right] \tag{33}$$

where the sum over $q$ is over all normal modes, $g_{kkq}$ is the force term in Eq. 23 transformed into the normal mode and eigenstate basis, and the sum over $k$ is over eigenstates of $H_{el}$. The polaron transform renormalizes the electronic energies

$$\tilde{\varepsilon}_k = \varepsilon_k - \sum_{q}\frac{g_{kkq}^2}{\omega_q} \tag{34}$$

and shifts the electronic coupling

$$\tilde{V}_{kk'} = \left(e^{-S}H_{el-ph}e^{S}\right)_{kk'}$$

$$= \sum_{k \neq k'}|k\rangle\langle k'|M_{kk'} \tag{35}$$

where

$$M_{kk'} = \sum_{q}g_{kk'q}\left(a_q^\dagger + a_q - \frac{2g_{kkq}}{\omega_q}\right)e^{\sum_{q'}\left(\frac{g_{kkq'} - g_{k'k'q'}}{\omega_{q'}}(a_{q'}^\dagger - a_{q'})\right)} \tag{36}$$

is the dressed off-diagonal coupling. Transforming to the Heisenberg representation and integrating over the phonon degrees of freedom leads to an expression for the golden-rule rate in terms of the autocorrelation of these dressed operators

$$W_{kk'} = 2\text{Re}\int_0^\infty \sum_{qq'}Tr\left[M_{kk'q}M_{k'kq'}(t)\rho_{eq}^{ph}\right]e^{-i(\tilde{\varepsilon}_k - \tilde{\varepsilon}_{k'})t}dt \tag{37}$$

In general, the time-correlation function has recurrences (since it is a sum of periodic functions) and in practice we perform the time iteration only over a sufficiently long enough interval for the correlation function to decay and truncate the integration before the first recurrence.

While this approach is accurate and we have used it extensively for computing rates, the drawback is that it is time-consuming to to compute this between each and every possible eigenstate of $H_{el}$ and then average over energetic fluctuations. Since we are primarily interested in transitions from a local exciton to charge-separated states, we developed a machine-learning approach to rapidly parse through the $H_{el}$ eigenstates and select only excitonic and charge-separated eigenstates using a training set of pre-determined exciton and charge-separated states.

Secondly, we wanted to understand whether or not the charge-separated/polaron states are entangled electron/hole polarons or if the state is separable into a product of polaron states. In other words, can we write a given charge-separated state given as a linear combination of site-local wavefunctions

$$\psi_k(r_e, r_h) = \sum_{ij}c_{ij}^k\phi_i(r_e)\overline{\phi}_j(r_h) \tag{38}$$

as a sum over a single index

$$\psi_k(r_e, r_h) = \sum_{n}\lambda_n^k f_n^k(r_e)g_n^k(r_h) \tag{39}$$
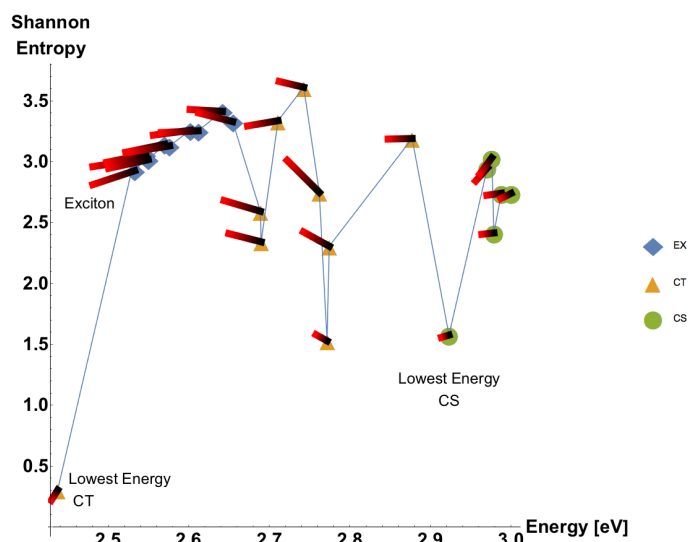
**Fig. 6** Correlation between state energy, Shannon entropy, and net flux from a given state for a model Heterojunction system.

where the $f_n^k(r_e)$ and $g_n^k(r_h)$ are orthogonal polynomials given by Schmidt decomposition of $\psi^k(r_e, r_h)$. These are the so-called "Schmidt modes" from quantum information theory. Using the normalized Schmidt eigenvalues $\tilde{\lambda}_n^k$ for a given eigenstate, we can define the Shannon entropy as

$$S_k = -\sum (\tilde{\lambda}_n^k)^2 \ln((\tilde{\lambda}_n^k)^2). \qquad (40)$$

When $S_k = 0$, only one term contributes to the sum (with only one of the $\tilde{\lambda}_k = 1$). Furthermore $S = \ln N$ where $N$ is dimensionality of the information space needed to describe a given eigenstate. In essence, $N = \exp(S)$ gives the minimum number of single-particle reducible states needed to describe a given many-body wavefunction. For an entangled two particle wavefunction as given in Eq. 38, that decomposition is expressed in Eq. 39. If $S = 0$, only one term will contribute to this sum, and the CI eigenstate would be a simple product of a single valance-band electron orbital times a single conduction-band hole orbital. Consequently, one anticipates that localized polaron states would be states with minimal entanglement and hence describable as separable electron/hole states and excitonic states to be highly entangled and generally non-separable.

In Figure 6 we compare the state energy and its associated entropy for a given lattice realization. Here we determined whether a given eigenstate is charge-separated (green dots), charge-transfer (yellow triangles), or excitonic (blue diamonds) using a machine learning method that compared computed electron/hole eigenstates to "idealized" CS, CT, or excitonic states. For clarity we show the results from only a single lattice realization. First, we note that excitonic states tend to cluster with high entanglement entropies which one anticipates since the the electron and hole are occupying the same set of sites on the lattice. Similarly, the lowest energy CT state, which is best described as an electron/hole pair separated across the interface, but pinned to each other via Coulombic interactions. Interestingly, even though their center of mass motions are coupled, the state itself is separa-

ble into a product of polaron states. Energetically above the excitons lie another band of charge-transfer states. While these states are CT in character, the electron and hole remain highly entangled and in general these states contain some excitonic configurations. Finally, energetically above these are true charge-separated states; however, Schmidt decomposition reveals that these are not strictly separable into electron and hole single-particle polaron states.

Figure 6 also shows the net rate that population leaves a given energy state

$$\eta_n = \sum_i (W_{in} - W_{ni}) \qquad (41)$$

as indicated by a flag whose magnitude indicates the magnitude of $\eta_n$ and whose direction indicates the flow on the $(E, S)$ plane. Not surprisingly, the net "flow" is towards the lowest energy CT state. However, it is interesting to note that the lowest energy CS state is a kinetic trap.

## 3 Conclusions

In this work, we have discussed various approaches we have followed to connect the interfacial energetics to the observed open-circuit voltage for organic polymer-based photovoltaic cells. Such coarse-grained models provide considerable insight into to the energetics and kinetics of charge-transfer processes in mesoscale systems that are currently too large to be considered using more atomistic/ab initio based models. In particular, this discussion has focused upon the role of the density of states and entropic contributions to the charge-separation process following photoexcitation. One of the principle results of this analysis is a comparison between an analytical model based upon the Wigner-Weisskopf model for the decay of a quantum state into a broad continuum to a more detailed lattice model our group has developed. Surprisingly, the two models give remarkably similar results in the limit that the mobility of the transferred charge is sharply reduced in the direction perpendicular to the interface.

Secondly, we test the hypothesis that the charge-separated state is a simple product of a electron and a hole state of the form

$$\psi_{cs}(r_e, r_h) = \phi_e(r_e)\phi_h(r_h).$$

In other words, that the singular value decomposition of the full electron/hole wave function of Eq. 38 should contain exactly one and only one non-trivial term in Eq. 39 resulting in a a Shannon entropy (Eq. 40) of exactly 0. Rather, we find that only the lowest energy CT state is the least entangled electron/hole state. We shall continue to explore the connection between dissociated CS states and their Shannon entropy since it pertains as to the range at which electrons and holes are truely separable species.

## Acknowledgements

# References

1 M. D. Chatzisideris, A. Laurent, G. C. Christoforidis and F. C. Krebs, *Appl. Energy*, 2017, **208**, 471 – 479.

2 S. H. Park, A. Roy, S. Beaupre, S. Cho, N. Coates, J. S. Moon, D. Moses, M. Leclerc, K. Lee and A. J. Heeger, *Nat. Photonics*, 2009, **3**, 297–302.

3 M. Scharber and N. Sariciftci, *Prog. Polym. Sci.*, 2013, **38**, 1929 – 1940.

4 Z. He, B. Xiao, F. Liu, H. Wu, Y. Yang, S. Xiao, C. Wang, T. P. Russell and Y. Cao, *Nat. Photonics*, 2015, **9**, year.

5 S. Gélinas, A. Rao, A. Kumar, S. L. Smith, A. W. Chin, J. Clark, T. S. van der Poll, G. C. Bazan and R. H. Friend, *Science*, 2014, **343**, 512–516.

6 A. C. Jakowetz, M. L. Böhm, J. Zhang, A. Sadhanala, S. Huettner, A. A. Bakulin, A. Rao and R. H. Friend, *J. Am. Chem. Soc.*, 2016, **138**, 11672–11679.

7 B. A. Gregg, *J. Phys. Chem. Lett.*, 2011, **2**, 3013–3015.

8 S. N. Hood and I. Kassal, *J. Phys. Chem. Lett.*, 2016, **7**, 4495–4500.

9 T. M. Burke, S. Sweetnam, K. Vandewal and M. D. McGehee, *Adv. Energy Mater.*, 2015, **5**, 1500123.

10 S. Karabunarliev and E. R. Bittner, *The Journal of Chemical Physics*, 2003, **119**, 3988–3995.

11 S. Karabunarliev and E. R. Bittner, *The Journal of Physical Chemistry B*, 2004, **108**, 10219–10225.

12 E. R. Bittner, J. G. S. Ramon and S. Karabunarliev, *Journal of Chemical Physics*, 2005, **122**, 214719–214719.

13 E. R. Bittner, J. G. S. Ramon and S. Karabunarliev, *The Journal of Chemical Physics*, 2005, **122**, 214719.

14 E. R. Bittner, S. Karabunarliev and A. Ye, *The Journal of Chemical Physics*, 2005, **122**, 034707.

15 S. Karabunarliev and E. R. Bittner, *The Journal of Chemical Physics*, 2003, **118**, 4291–4296.

16 S. Karabunarliev and E. R. Bittner, *Phys. Rev. Lett.*, 2003, **90**, 057402.

17 V. Lankevich and E. R. Bittner, *Journal of Chemical Physics*, 2018, **149**, 244123.

18 A. Pereverzev and E. R. Bittner, *The Journal of Chemical Physics*, 2006, **125**, 104906.